Active versus passive control of vehicle suspensions - hardware in the loop experiments

K.J.Rieger and W.Schiehlen
University of Stuttgart, Germany

SYNOPSIS Hardware–in–the–loop simulation is shown to be a valuable tool for designing and testing controllers for active vehicle suspensions. The vehicle is modeled as a multibody system, whereas the electronic and hydraulic parts of the suspension are actuated on a test bed. A comparison between an active and a passive suspension shows higher performance of the active suspension with respect to low frequency excitation.

NOTATION

y	vector of generalized coordinates
z	first derivative of y
z	performance variables
k	vector of generalized coriolis and centrifugal forces
q	vector of applied forces
x	state vector
x_S	transformed state vector
A	system matrix
b	control input vector
e	disturbance vector
J	optimization criteria
P	solution of Ricatti equation
m	mass
c	stiffness
d	damping coefficient
u	excitation
Δs	displacement of suspension
$\dot{s}$	displacement velocity of suspension

1 INTRODUCTION

New concepts for vehicle design are characterized by a strong impact of controlled components like actively controlled suspensions. The interaction between the mechanical parts of a vehicle and the electronic parts results in a strongly coupled mechatronic system. The mechanical parts are most reliable due to the long history of vehicle engineering while this is not the case for the electronic components. Therefore, there is a special need for testing the electronic components under realistic loading conditions. This can be achieved e.g. by road tests which are rather expensive and time consuming. Another possibility is to model the mechanical parts of the vehicle as a multibody system and include the electronic and hydraulic parts as hardware in the analysis. The dynamics of the vehicle is then completely known depending on the mechanical parameters of the system and the geometry of the test roads given. An analysis of the overall system can be performed by interfacing the electronic components to a real–time simulation of the mechanical parts. This concept is known as hardware–in–the–loop simulation.

However, even a properly designed actively controlled suspension will be more expensive than a traditional passive suspension, and therefore, the question has to be answered if the improvements achieved by active control are honored by the customer. A first answer may be given by pure vehicle dynamics simulations where performance criteria can be used to rate the vehicle behavior. More realistic, however, are hardware–in–the–loop simulations.

In this paper, the high-dynamic test bed for dampers and actuators available at the Institute B of Mechanics is used to evaluate the degree of improvement. A front wheel suspension unit of a comfortable middle-class car is compared with a force-controlled hydraulic actuator, both implemented in a quarter car model with a simplified McPherson suspension. Linear optimal control theory is used to design the fully active suspension.

2 HARDWARE-IN-THE-LOOP SIMULATION

In the dynamics of vehicle systems the approach of multibody systems is most appropriate. The vehicles are modeled as rigid bodies interconnected by constraint elements like joints and bearings and by coupling elements like springs, dampers or force-controlled actuators. The method of multibody systems has been developed during the last three decades and its theory is well established in the literature, e.g. SCHIEHLEN [1]. Using a minimal set of f generalized coordinates for describing the kinematics of the system, a compact and efficient formulation of the equations of motion can be obtained where f denotes the number of degrees of freedom. With the $f \times 1$ vector of generalized coordinates $\boldsymbol{y}$ and its first time derivative $\boldsymbol{z}$ the equations of motion of holonomic systems can be written as

$$\dot{\boldsymbol{y}} = \boldsymbol{z}\,,$$
$$\boldsymbol{M}(\boldsymbol{y},t)\,\dot{\boldsymbol{z}} + \boldsymbol{k}(\boldsymbol{y},\boldsymbol{z},t) = \boldsymbol{q}(\boldsymbol{y},\boldsymbol{z},t)\,. \tag{1}$$

Here, $\boldsymbol{M}$ denotes the symmetric and positive definite $f \times f$ inertia matrix, the $f \times 1$ vector $\boldsymbol{k}$ contains the generalized coriolis and centrifugal forces and the $f \times 1$ vector $\boldsymbol{q}$ contains the generalized applied forces. The modeling of multibody systems can be supported by computer formalisms such as the program NEWEUL, KREUZER and LEISTER [2]. For real-time implementation of the symbolic equations of motion on transputer networks special interfaces have been developed, SCHÄFER [3].

The dynamical system described in Eq. (1) consists only of the mechanical components. To describe the behavior of a mechatronic system, the dynamics of controlled elements exerting forces and torques on the mechanical parts have to be taken into account as well. An additional set of equations describing the dynamics of the controlled elements have to be added to Eq. (1), and additional parameters have to be determined by means of extensive measurements.

In an alternative approach for the analysis of mechatronic systems the simulation model of the overall system is replaced by a hardware-in-the-loop model. Instead of modeling the dynamics of actuators and control devices, these components are operated in an experimental set-up and the coupling to the multibody system is achieved by hardware-software interaction. The structure of such a hardware-in-the-loop model for an active suspension control is shown in Fig. 1.

It can be seen that the loop formed by the multibody system model and the test hardware contains an interface assembly that is needed to provide the actual motion input to the hardware parts of the model. This functional structure imposes strict requirements on the dynamic behavior of the test bed itself, as it has a major influence on the quality of the simulation results. The force-controlled actuator is mounted in the test rig with compliant supports as used in realistic vehicle suspensions. A load cell provides the force measurement for the force feedback and the hardware-in-the-loop simulation.

Hardware-in-the-loop modeling is a hybrid approach that requires the development of real-time simulation models of multibody systems on one hand, and the development of appropriate test rigs and hardware-software interfaces for the operation of actuator and control devices on the other hand. Once a test bed for a certain type of control device is established, a whole variety of systems can be investigated without considering the dynamic behavior of the hardware components in detail.

The main functional unit of the hydraulic test bed for hardware-in-the-loop testing of suspension elements is a position-controlled servo system. It generates the motion input for a force-controlled hydraulic suspension actuator. The position servo system consists of a high-performance symmetrical, double-ended hydraulic cylinder with integrated displacement sensor. It is controlled by two two-stage, high-response servo-valves operating in parallel. Thus, the oil flow required for the maximum piston velocity can be provided with smaller valves having considerably higher bandwidth than a single valve with double nominal flow. Another design measure for improving dynamic properties is the use of an external pressure supply for the pre-stage of the servo-valves so that supply pressure fluctuations caused by fast motion patterns will have no influence on the servo-valve behavior. Accumulators in supply and return pipes further reduce dynamic pressure changes. Pressure sensors provide measurements of supply and piston chamber pressures for control purposes.

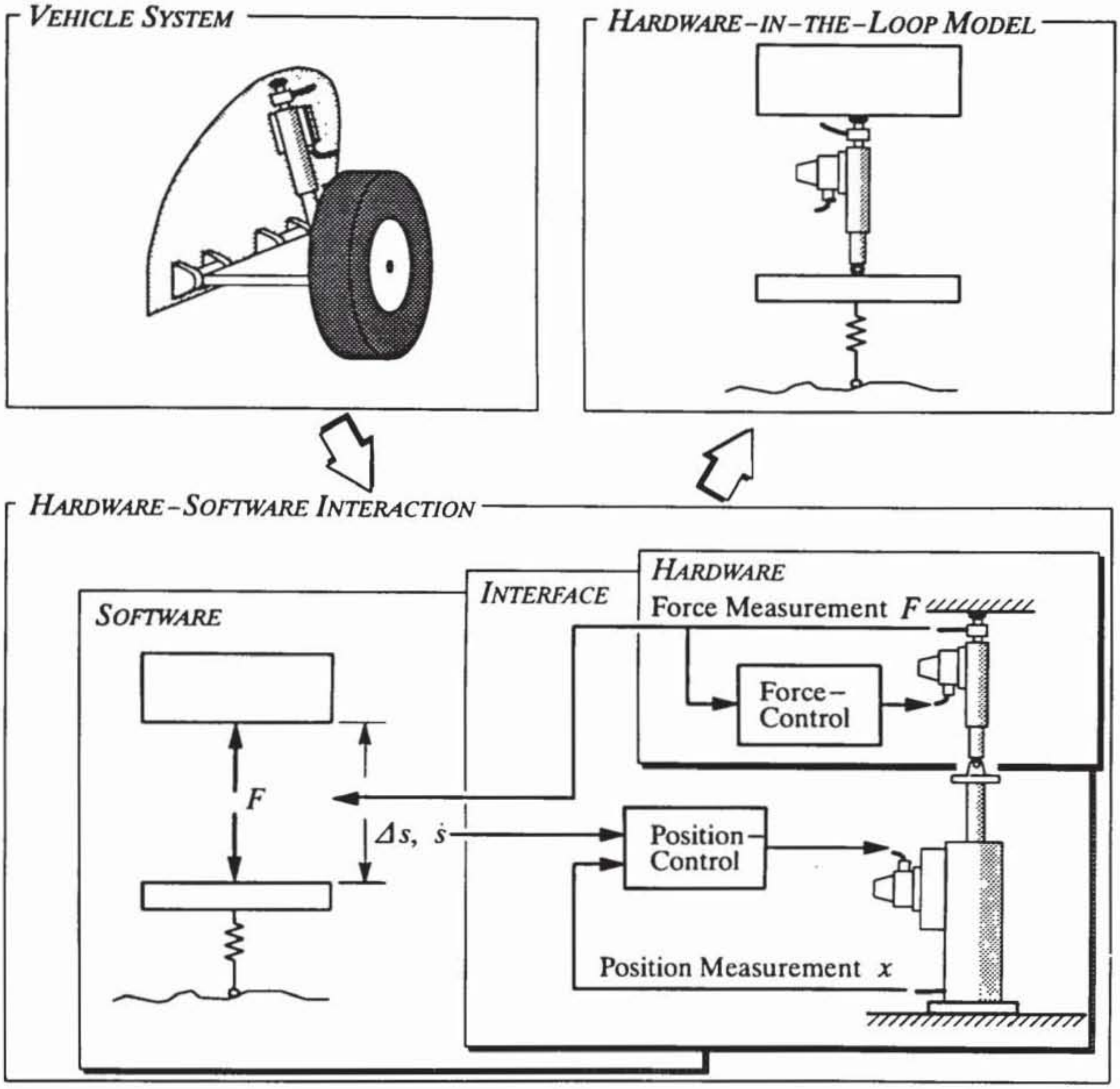

Figure 1: Hardware-in-the-loop model of an active vehicle suspension

As already mentioned before, the dynamic behavior of the test bed has a major influence on the quality of the simulation results. Especially, phase lag of the cylinder has a severe impact on the quality of the simulation because it is fed back into the simulation model. But due to a control design which consists of two parts, a linear quadratic regulator approach and a phase lag compensation, the system shows an excellent phase behavior up to approximately 35 Hz. This is fully sufficient for covering body and wheel modes of suspension motion.

The components described above are supported by a hydraulic pressure supply unit with a variable displacement pump for the main supply, a fixed displacement pump for the pre-stage supply, and various components and valves for heating and cooling of the hydraulic fluid and for control and safety features.

The power control unit is connected with peripheral interfaces of a transputer system for digital control and real-time simulation. A graphics workstation is used for data monitoring and operator interaction.

3 VEHICLE MODEL

To have a realistic comparison between passive and active suspensions a quarter car model with a simplified spatial McPherson suspension is used, see Fig. 2.

The masses of body and wheel are m_b and m_w, respectively. The suspension is represented by the force input F measured at the hardware element. The tire elasticity is described by a linear spring with stiffness c_w. The road profile is described by the coordinate u_r, whereas α and x_w are used for describing the body and wheel motion, respec-

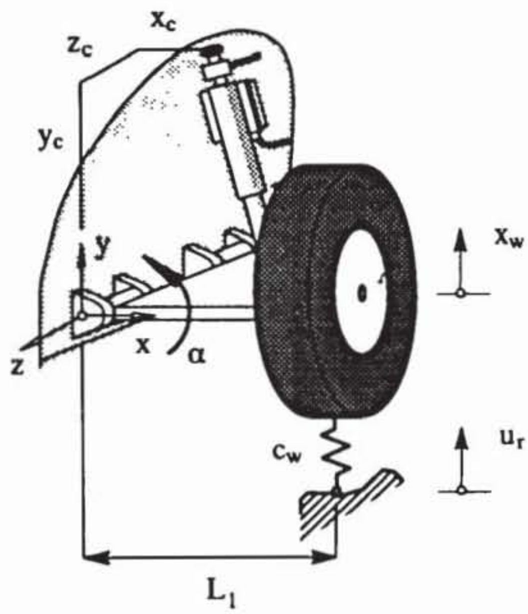

Figure 2: McPherson suspension

tively. Supported by the computer formalism NEWEUL, KREUZER and LEISTER [2] the equations of motion are obtained as

$$\ddot{a} = \frac{-(m_b + m_w)\, F_H \cos(a - \gamma) + m_b c_w (u_r - x_w) \cos a}{m_b L_1 (m_w + m_b \sin^2 a)} \quad (2)$$

$$\ddot{x}_w = \frac{c_w(u_r - x_w) - F_H \cos a \cos(a - \gamma)}{m_w + m_b \sin^2 a} \quad (3)$$

where

$$\gamma = \arctan \left[\frac{\sqrt{z_c^2 + (L_1 \cos a - x_c)^2}}{y_c - L_1 \sin a} \right]. \quad (4)$$

The geometrical data are found in Table 1.

Table 1 Geometrical data

xc	0.2075 *m*
yc	0.52 *m*
zc	0.1 *m*

For the control input of the test bed the displacement Δs and the velocity $\dot{s}$ of the suspension are needed. They are obtained as

$$\Delta s = \frac{y_c - L_1 \sin a}{\cos \gamma} - \frac{y_c - L_1 \sin a_0}{\cos \gamma_0} \quad (5)$$

$$\dot{s} = \frac{L_1}{s} (x_c \sin a - y_c \cos a)\, \dot{a} \quad (6)$$

where the length of the actuator is

$$s = \sqrt{z^2 + x^2 + y^2 + L_1^2 - 2 L_1 (x_c \cos a + y_c \sin a)} \quad (7)$$

and γ_0 and a_0 are initial values.

4 CONTROL DESIGN

Generally, the task of a suspension is to gently absorb inputs from the road surface and actively suppress vehicle attitude changes so as to eliminate any excess vehicle motion to get maximum ride comfort and optimal handling performance. It should provide such performance regardless of perturbations or roughness in the road surface and loading conditions. On the other hand, wheel load fluctuations should be as small as possible for ride safety reasons.

Obviously, the design of a suspension can only be a compromise between ride comfort and ride safety. To fulfill the requirements for the control design of an active suspension which are

- stable system,
- easy to understand control structure,
- and fast and reliable implementation,

the vehicle controller has to be split into two hierarchical levels. The task of the decentral part is the force control. It is needed to stabilize the actuator and to feedback the suspension displacement. The central part gets information about car velocity, steering angle and angular velocity etc. Its task is to selectively damp wheel and body motion.

The control design is splitted into two parts. Firstly, a force–controller for the actuator will be designed. This corresponds to the decentral part mentioned before. Secondly, linear optimal control theory is applied to design a fully active suspension. where the dynamics of the actuator is neglected. The active suspension is then implemented into a quarter car model with a simplified McPherson suspension and simulated within the hardware–in–the–loop simulation set–up.

4.1 Force Control Design

For the purpose of controller design a mathematical model of the actuator has to be generated. The modeling of hydraulic servo systems is presented in detail e.g. in BACKÉ [4] or MERRITT [5]. The force–controlled actuator used as active suspension element consists of a single–ended cylinder and a two–stage servo–valve. It is mounted in the test rig with compliant support as used in realistic vehicle suspensions.

Fig. 3 shows an idealized single–ended piston controlled by a servo–valve. The piston is characterized by the piston area A_p and the ring area A_r. The cylinder mass is m_c. The cylinder is fixed to the test rig by a rubber buffer with the stiffness c_c and the damping coefficient d_c. Resisting forces due to leakage flow and friction are taken into account by a viscous damping coefficient d_H. The flow through the servo–valve control ports C_A and C_B is denoted by q_A and q_B, and the leakage flow between the piston chambers is q_{Li}. The coordinates x_c and y denote the cylinder displacement and the servo–valve spool displacement, respectively, and p_A and p_B denote the piston chamber pressures. The coordinate u_p denotes the displacement input to the actuator.

The dynamic model of the actuator is given by the equations of motion of the cylinder, the servo–valve spool and additional differential equations for the piston chamber pressures. A major nonlinearity results from the nonlinear characteristic of the servo–valve orfice flow. Linearizing about mid–stroke position and applying additional assumptions about the leakage flow finally leads to the linear state equation

$$\dot{x} = A\,x + b\,u_V + e\,r \tag{8}$$

with the 6×1 state vector

$$x = \left[\, y,\, y,\, p_A,\, p_B,\, x_c,\, x_c \right]^T . \tag{9}$$

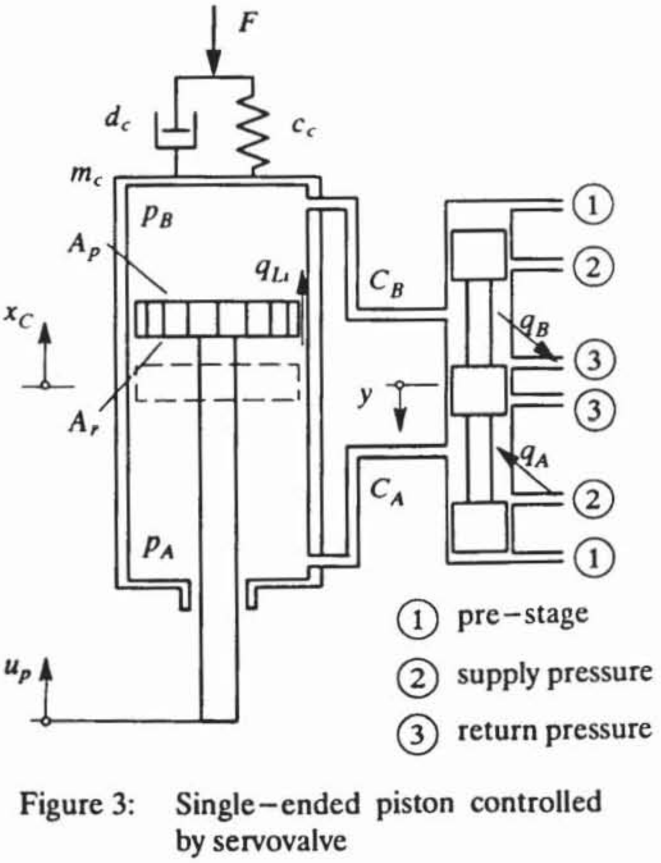

Figure 3: Single–ended piston controlled by servovalve

The scalar control input u_V is given by the servo–valve input. The disturbance input $r = [\dot{u}_p]$ contains the external velocity input. The 6×6 system matrix A is given by

$$A = [a_1 \;...\; a_6]$$

$$a_1 = \left[\, 0,\, -\omega_V^2,\, -\frac{V_{qy}}{C_{H,A}},\, \frac{V_{qy}}{C_{H,B}},\, 0,\, 0\right]^T$$

$$a_2 = \left[1,\, -2D_V\,\omega_V,\, 0,\, 0,\, 0,\, 0\right]^T$$

$$a_3 = \left[0,\, 0,\, -\frac{k_p - V_{qy}}{C_{H,A}},\, \frac{k_p}{C_{H,B}},\, -\frac{A_r}{m_c},\, 0\right]^T$$

$$a_4 = 0,\, 0,\, \frac{k_p}{C_{H,A}},\, -\frac{k_p - V_{qy}}{C_{H,B}},\, -\frac{A_p}{m_c},\, 0]^T$$

$$a_5 = \left[0,\, 0,\, 0,\, 0,\, -\frac{c_c}{m_c},\, 0\right]^T$$

$$a_6 = \left[0,\, 0,\, \frac{A_r}{C_{H,A}},\, -\frac{A_p}{C_{H,B}},\, -\frac{d_c - d_H}{C_{H,B}},\, 1\right]^T. \tag{10}$$

The system parameters are the servo–valve eigenfrequency ω_V, the damping ratio D_V, the leakage flow coefficient k_p, the flow gain V_{qy}, and the flow–pressure coefficient V_{qp}. The hydraulic capacities C_{HA} and C_{HB} of chamber A and B are determined by the efficient bulk modulus E_H of the hydraulic fluid and the efficient volume V_A and V_B, respectively, i.e. $C_{HA,B} = V_{A,B}/E_H$. Finally, the control input vector is given by

$$b = \left[\, \omega_V^2 k_V,\, 0\,,\, 0\,,\, 0\,,\, 0\,,\, 0\right]^T \tag{11}$$

where k_V denotes the servo–valve gain, and the disturbance input is characterized by

$$e = \left[0\,,\, 0\,,\, -\frac{A_r}{C_{H,A}}\,,\, \frac{A_p}{C_{H,B}}\,,\, 0\,,\, 0\right]^T . \tag{12}$$

With a simple proportional force–feedback a good reference behavior can be obtained but the disturbance behavior is unsatisfactory. Because of the high force gain of the hydraulic cylinder only small apertures of the servo–valve are required to generate large force alternations. On the other hand, fast motions of the piston demand large oil flows which can only be applied by large apertures and therefore large force deviations. Therefore, a good force control characteristic can be obtained as long as the piston doesn't move whereas piston motion yields unacceptable force deviations.

To solve the problem a servo–valve spool displacement according to the flow required for a quasistatic motion of the piston with the actual velocity can be introduced as an additional control input. The resulting controller consists of two parts. The first part is of the type PID_{T1} whereas the second part is the velocity compensation. The digital control is implemented on a transputer system. The servo–valve input is obtained as

$$u_V = K_p\, e_K + y_{I,K} + y_{D,K} + K_{ZA}\, u_p \qquad (13)$$

where K_{ZA} denotes the disturbance velocity gain factor.

The frequency response of the closed loop system is given in Fig. 4.

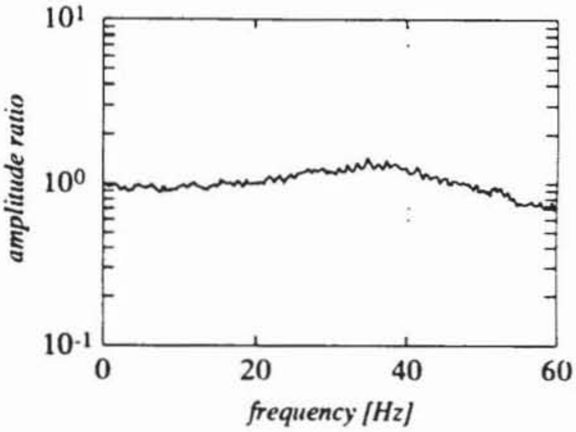

Figure 4: Frequency response of the force–controlled actuator

4.2 Active Suspension Design

The design of the central suspension controller is based on the paper of WILSON et. al. [7]. For the design of the controller a linear system with two degrees of freedom and full state feedback is considered, Fig. 5.

The dynamic model is given by the equations of motion of the wheel and the body of the car:

$$\dot{x} = A\,x + b\,u_F + e\,v\,, \qquad (14)$$

$$z = C\,x \qquad (15)$$

with the 5×1 state vector

$$x = [\,u_r, x_w, x_b, \dot{x}_w, \dot{x}_b]^T\,. \qquad (16)$$

The scalar control input u_F is given by the force of the hydraulic actuator and v represents a single white noise disturbance input. The 5×5 system matrix A is given by

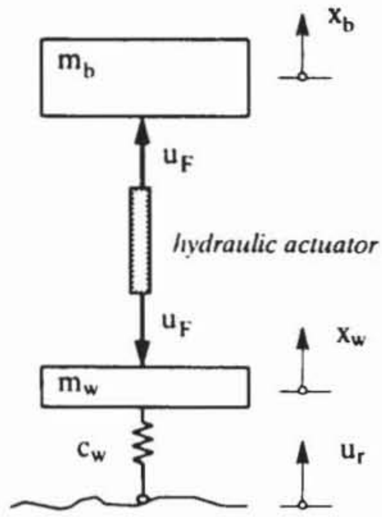

Figure 5: Quarter car active suspension system

$$A = \begin{bmatrix} 0 & 0 & 0 & 0 & 0 \\ 0 & 0 & 0 & 1 & 0 \\ 0 & 0 & 0 & 0 & 1 \\ a & -a & 0 & 0 & 0 \\ 0 & 0 & 0 & 0 & 0 \end{bmatrix} \qquad (17)$$

where $a = c_w/m_w$. The 5×1 control input vector reads as

$$b = \left[\,0\,,\,0\,,\,0\,,\,-\frac{1}{m_w}\,,\,\frac{1}{m_b}\,\right]^T. \qquad (18)$$

The variables chosen for the performance index are related to the state variables by

$$z = \begin{bmatrix} -1 & 1 & 0 & 0 & 0 \\ 0 & -1 & 1 & 0 & 0 \end{bmatrix} x = C\,x\,. \qquad (19)$$

Since this system has one uncontrollable and one unobservable mode, it has to be transformed using Thompson's transformation which reads as

$$x_S = S\,x \qquad (20)$$

where

$$S = \begin{bmatrix} 1 & 0 & 0 & 0 & 0 \\ -1 & 1 & 0 & 0 & 0 \\ -1 & 0 & 1 & 0 & 0 \\ 0 & 0 & 0 & 1 & 0 \\ 0 & 0 & 0 & 0 & 1 \end{bmatrix}. \qquad (21)$$

The state equation is then given by

$$\dot{x}_S = S\,A\,S^{-1}\,x_S + S\,b\,u_F + S\,r\,v\,, \qquad (22)$$

$$z = C\,S^{-1}\,x_S\,. \qquad (23)$$

The uncontrollable mode associated with the road surface displacement $x_{S1} = u_r$ has now become unobservable as well, and the feedback law then only depends on $x_{S2} \ldots x_{S5}$. The sub–problem obtained by striking out the first row of Eqns. (22) and (23), respectively, is stabilizable and detectable. With the solution of the Ricatti equation

$$\bar{A}^T P + P\bar{A} + \bar{C}^T Q \bar{C} - P\bar{B}R^{-1}\bar{B}^T P = 0 \qquad (24)$$

the control law is given by

$$u_F = -R^{-1}\bar{B}^T P\, x_S \qquad (25)$$

which is optimal with respect to

$$J = \int_0^\infty (\, z^T Q\, z + u_F^T R\, u_F \,)\, dt \qquad (26)$$

where $Q = diag\{q_1\ q_2\}$ and $R = 1$. The weighting factor R is related to ride comfort, the factors q_1 and q_2 correspond to tyre load fluctuations and suspension working space requirements, respectively.

For the system parameters

$$m_b = 335\ kg,\ \ m_w = 25\ kg,\ \ c_w = 250000\ \frac{N}{m}$$

and the weighting coefficients $q_1 = 6.075 \times 10^{10}$ and $q_2 = 2.025 \times 10^6$ the frequency responses in Fig. 6 are obtained. The upper graph shows the carbody acceleration rated by a filter which takes into consideration the human feeling for discomfort, e.g. POPP and SCHIEHLEN [8]. The lower graph shows the tire load fluctuations as a measure for ride safety.

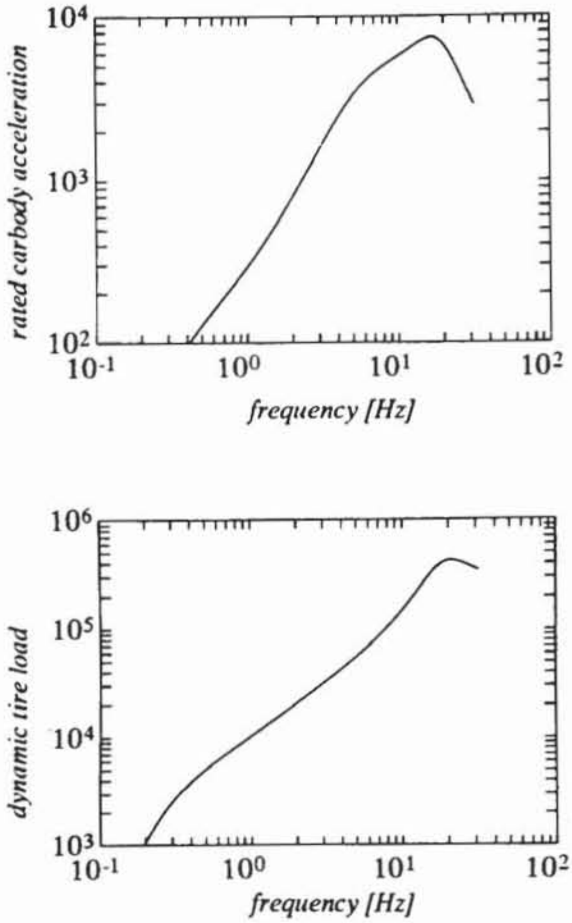

Figure 6: Computed frequency response of the rated carbody acceleration and tire load fluctuations

5 EXPERIMENTAL RESULTS

To compare the active suspension on the basis of the controllers developed in the previous section to passive suspensions, the front wheel suspension of a comfortable middle–class car was mounted on the test rig. For obtaining realistic results the damper and spring of the suspension was mounted to the test rig with the original bearings.

Both the passive and the active suspension where analyzed within the hardware–in–the–loop simulation set–up in combination with the quarter car model described in section 3. Fig. 7 shows the frequency responses of the rated carbody accelerations and the tire load fluctuations.

A comparison with Fig. 6 shows good agreement of the experimental results with the theoretical results. The small deviations at low frequencies, however, show that it is advisable to complement theoretical investigations by hardware–in–the–loop experiments. It has to be noted that such a good agreement could only be achieved by properly tuning the force controller within the hardware–in–the–loop set–up. Other experiments have pointed out much more that the dynamic behavior of a real hydraulic actuator differs from the behavior of simulation models.

Obviously, the active suspension offers more ride comfort with respect to the frequency band around the eigenfrequency of the carbody whereas nothing can be gained for high frequencies. Also ride safety can be improved at this bandwidth at the expense of rather small deteriorations at high frequencies. Additional experiments with different control laws have shown that comfort can be further improved if higher tire load fluctuations are acceptable in the frequency range around the wheel eigenfrequency.

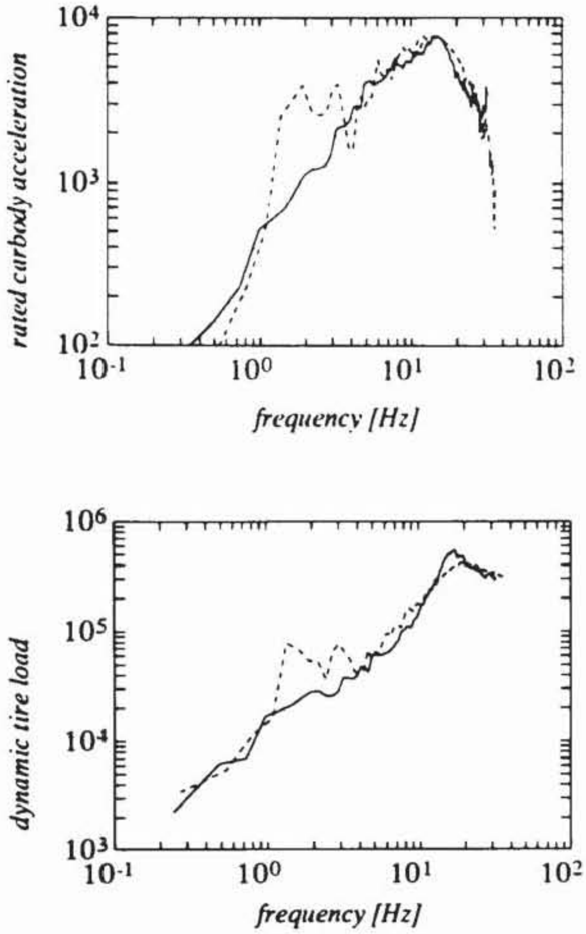

Figure 7: Experimental frequency response of the rated carbody acceleration and tire load fluctuations (__ actice suspension, _ _ passive suspension)

CONCLUSIONS

In this paper, a hardware-in-the-loop simulation set-up for passive and active vehicle suspension analysis and design is described. A shock absorber of a middle-class car is compared with an actively controlled suspension in combination with the software model of a quarter car with a simplified McPherson suspension. The controller of the active hydraulic strut consists of a force controller and a suspension control strategy on a higher level which is designed via linear optimal control theory. The comparison shows that ride comfort and safety can be improved especially for low frequencies if passive suspensions are replaced by hydraulic actuators.

REFERENCES

[1] SCHIEHLEN, W., *Technische Dynamik*. Stuttgart: Teubner, 1986.

[2] KREUZER, E., LEISTER, G., *Programmsystem NEWEUL '90, Anleitung*. Stuttgart: Universitat, Institut B fur Mechanik, Anleitung AN-23, 1991.

[3] SCHAFER, P., *Echtzeitsimulation von Mehrkörpersystemen auf Transputernetzwerken*. Dissertation. University of Stuttgart, Institute B of Mechanics. (To appear).

[4] BACKÉ, W., *Servohydraulik*. Course manuscript. Aachen: Rheinisch-Westfälische Hochschule, Institut fur hydraulische und pneumatische Antriebe und Steuerungen, 1992.

[5] MERRITT, H. E., *Hydraulic Control Systems*. New York: Wiley & Sons, 1967.

[6] FEIGEL, H.-J., Nichtlineare Effekte am servoventilgesteuerten Differentialzylinder. *o+p Oelhydraulik und Pneumatik*, **1**, 1987, 42-48.

[7] WILSON, D. A., SHARP, R. S., HASSAN, S. A., The Application of Linear Optimal Control Theory to the Design of Active Automotive Suspensions. *Veh. Sys. Dyn.*, **15**, 1986, 105-118.

[8] POPP, K., SCHIEHLEN, W., *Fahrzeugdynamik*. Stuttgart: Teubner, 1993.